Coherent Optics

Advanced Texts in Physics

This program of advanced texts covers a broad spectrum of topics which are of current and emerging interest in physics. Each book provides a comprehensive and yet current and emerging interest in physics. Each book provides a comprehensive and yet accessible introduction to a field at the forefront of modern research. As such, these texts are intended for senior undergraduate and graduate students at the MS and PhD level; however, research scientists seeking an introduction to particular areas of physics will also benefit from the titles in this collection.

Springer
Berlin
Heidelberg
New York
Hong Kong
London
Milan
Paris
Tokyo

Physics and Astronomy ONLINE LIBRARY
http://www.springer.de/phys/

W. Lauterborn T. Kurz

Coherent Optics

Fundamentals and Applications

Second Edition
With 183 Figures,
73 Problems and Complete Solutions

Springer

Professor Dr. Werner Lauterborn
Dr. rer. nat. Thomas Kurz
Universität Göttingen
Drittes Physikalisches Institut
Bürgerstrasse 42–44
Germany

Title of the original German edition:
W. Lauterborn, T. Kurz, and M. Wiesenfeldt: Kohärente Optik
ISBN 3-540-56769-0

Library of Congress Cataloging-in-Publication Data applied for.
Die Deutsche Bibliothek - CIP-Einheitsaufnahme
Lauterborn, Werner:
Coherent optics: fundamentals and applications/W. Lauterborn; T. Kurz. –
2. ed. – Berlin; Heidelberg; New York; Hong Kong; London; Milan; Paris; Tokyo:
Springer, 2003 (Advanced texts in physics)
(Physics and astronomy online library)
Einheitssacht.: Kohärente Optik <engl.>
ISBN 3-540-43933-1

ISSN 1439-2674

ISBN 3-540-43933-1 2nd Edition Springer-Verlag Berlin Heidelberg New York

ISBN 3-540-58372-6 1st Edition Springer-Verlag Berlin Heidelberg New York

Springer-Verlag Berlin Heidelberg New York
a member of BertelsmannSpringer Science+Business Media GmbH

http://www.springer.de

Printed in Germany

Typesetting: Data prepared by the author using a Springer TEX macro package
Cover design: *design & production* GmbH, Heidelberg

Printed on acid-free paper SPIN 10646913 56/3141/tr 5 4 3 2 1 0

5. Multiple-Beam Interference

When discussing the coherence properties of light, we mainly compared two light waves with each other. In the course of deriving the condition for spatial coherence, we in fact considered light sources comprising many independent point sources. Their waves, however, were incoherently summed by adding the intensities. We now consider phenomena occurring when many mutually coherent waves are superimposed: multiple-beam interference. To them belong Newton's rings, the color of thin films, Bragg reflection, and also the principle underlying interference filters. An important instrument, whose operation is based on multiple superposition of light waves, is the Fabry–Perot interferometer.

5.1 Fabry–Perot Interferometer

The operation of a Fabry–Perot interferometer has been known since more than a hundred years. But it is by no way an obsolete device. It makes use of multiple-beam interference and has many applications in modern optics. It serves as a device of extremely high resolution in spectroscopy, and, as a resonator, forms part of the laser.

A Fabry–Perot interferometer basically consists of just two plane parallel, highly reflecting surfaces together with some means to alter the distance between them (Fig. 5.1). In the form of a plane parallel glass plate made highly reflecting on both sides, it is called an etalon (Fig. 5.2).

The effect a Fabry–Perot interferometer has on a light wave comes about through the interference of the light waves that are reflected back and forth between the surfaces. To arrive at a mathematical description, we consider a plane wave propagating perpendicularly to the plane parallel mirrors, which are seperated by the distance L and have the same reflectance and the same transmittance.

We write the incoming plane wave in the complex form

$$E_\mathrm{e} = E_\mathrm{e}(z,t) = E_0 \exp\left(ikz - i\omega t\right) . \tag{5.1}$$

The wave reflected at one of the mirrors is denoted by E_r, the one transmitted by E_t. We do not consider the phase shifts that may occur upon

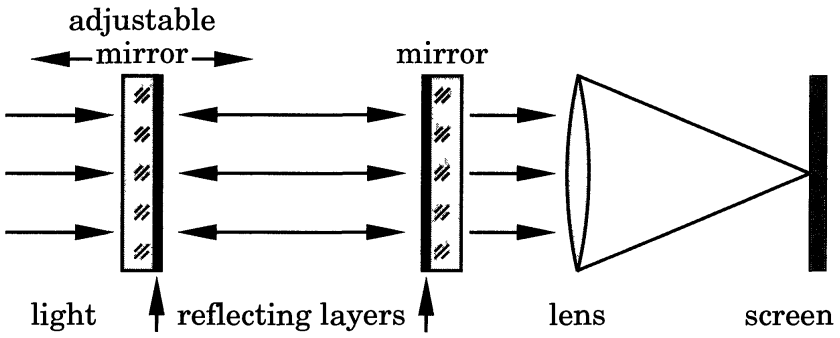

Fig. 5.1. Fabry–Perot interferometer.

reflection and transmission. They do not alter the principle of operation of the instrument. Then, the amplitude reflectance r and the amplitude transmittance t, defined by

$$r = \frac{E_r}{E_e} \quad \text{and} \quad t = \frac{E_t}{E_e}, \tag{5.2}$$

are real numbers between zero and one. Moreover, we suppose that the mirrors are nonabsorptive. Then, by the law of conservation of energy, the following relation holds:

$$r^2 + t^2 = 1. \tag{5.3}$$

With these assumptions, the electric field amplitude immediately behind the left mirror (see Fig. 5.3) after the incoming wave E_e has passed the first mirror is

$$E_t = tE_e(0,t) = tE_{e0}.$$

After passage of the light through the second mirror we have:

$$E_1 = tE_t \exp(ikL) = E_{e0}t^2 \exp(ikL). \tag{5.4}$$

Because of the optical path length L between the mirrors a phase factor $\exp(ikL)$ is introduced. Part of the wave $E_t \exp(ikL)$ incident on the

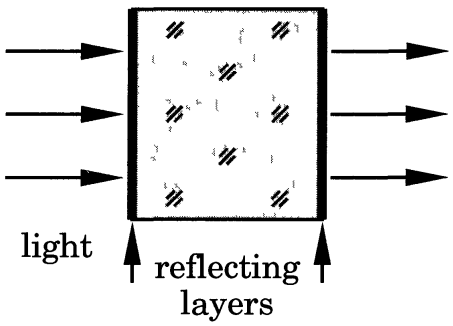

Fig. 5.2. Etalon.

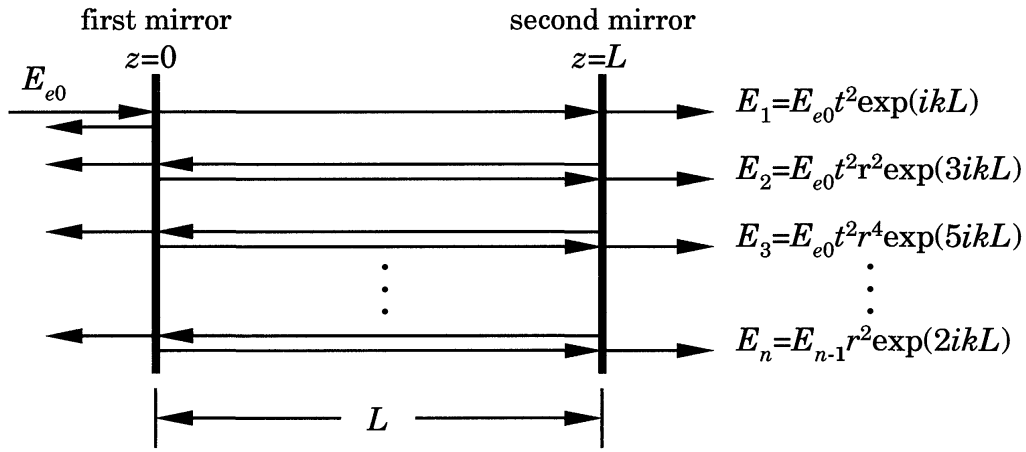

Fig. 5.3. Light waves in a Fabry–Perot interferometer.

second mirror is reflected, giving a wave

$$E_{1r} = trE_{e0}\exp(ikL)$$

traveling back to the first mirror. After additional reflection at the first mirror and passage through the second mirror, the amplitude

$$E_2 = E_{e0}t^2r^2\exp(ik3L) \tag{5.5}$$

is obtained. The output wave now has suffered two transmissions (t^2) and two reflections (r^2) and has experienced an additional phase shift $k3L$ because of the path length $3L$. From (5.4) and (5.5) the law for the partial waves being transmitted can immediately be derived. After each round trip the wave amplitude has to be multiplied by $r^2\exp(ik2L)$, giving

$$E_n = E_{n-1}r^2\exp(ik2L), \qquad n = 2,3,\ldots, \tag{5.6}$$

or, explicitly written:

$$E_n = E_{e0}t^2\exp(ikL)\,r^{2(n-1)}\exp[ik2(n-1)L]\,. \tag{5.7}$$

As we have assumed a plane wave, the partial waves E_1, E_2, E_3, ... superimpose behind the second mirror to yield the output wave amplitude E_t:

$$\begin{aligned} E_t &= \sum_{n=1}^{\infty} E_n = E_{e0}t^2\exp(ikL)\sum_{n=1}^{\infty} r^{2(n-1)}\exp[ik2(n-1)L] \\ &= E_{e0}t^2\exp(ikL)\sum_{n=0}^{\infty} r^{2n}\exp(ik2nL) \\ &= E_{e0}t^2\exp(ikL)\sum_{n=0}^{\infty}[r^2\exp(ik2L)]^n\,. \end{aligned} \tag{5.8}$$

The sum is a geometric series that can be expressed in closed form:

$$\sum_{n=0}^{\infty} q^n = \frac{1}{1-q} \quad \text{for} \quad |q|<1. \tag{5.9}$$

Therefore, with

$$q = r^2 \exp\left(ik2L\right), \tag{5.10}$$

the output amplitude of the instrument is

$$E_\mathrm{t} = E_{\mathrm{e}0} t^2 \exp\left(ikL\right) \frac{1}{1-r^2\exp\left(ik2L\right)}. \tag{5.11}$$

As always, we are able to see or measure only the intensity. To simplify the notation, we introduce the phase shift δ for one round trip between the mirrors:

$$\delta = k2L. \tag{5.12}$$

We then get for the output intensity:

$$\begin{aligned} I_\mathrm{t} &= E_\mathrm{t}E_\mathrm{t}^* = E_{\mathrm{e}0}E_{\mathrm{e}0}^* t^4 \frac{1}{(1-r^2\exp[i\delta])(1-r^2\exp[-i\delta])} \\ &= I_\mathrm{e} t^4 \frac{1}{1+r^4-r^2\exp[-i\delta]-r^2\exp[i\delta]} \\ &= I_\mathrm{e} t^4 \frac{1}{1+r^4-2r^2\cos\delta}, \end{aligned} \tag{5.13}$$

where $I_\mathrm{e} = E_\mathrm{e}E_\mathrm{e}^* = E_{\mathrm{e}0}E_{\mathrm{e}0}^*$ is the input intensity entering the instrument. This expression is usually given a different form. With the relation $\cos\delta = 1-2\sin^2(\delta/2)$ we obtain:

$$\begin{aligned} I_\mathrm{t} &= I_\mathrm{e} t^4 \frac{1}{1+r^4-2r^2(1-2\sin^2(\delta/2))} \\ &= I_\mathrm{e} t^4 \frac{1}{(1-r^2)^2+4r^2\sin^2(\delta/2)}. \end{aligned} \tag{5.14}$$

Now, recalling that $r^2+t^2=1$ leads to:

$$\begin{aligned} I_\mathrm{t} &= \frac{I_\mathrm{e}}{1+(2r/(1-r^2))^2\sin^2(\delta/2)} \\ &= \frac{I_\mathrm{e}}{1+K\sin^2(\delta/2)} = \frac{I_\mathrm{e}}{1+K\sin^2 kL}. \end{aligned} \tag{5.15}$$

The quantity

$$K = \left(\frac{2r}{1-r^2}\right)^2 \tag{5.16}$$

is called finesse coefficient.

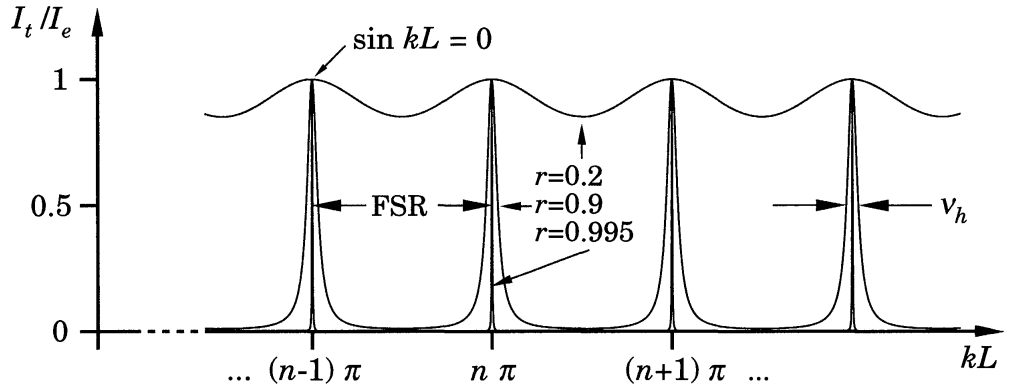

Fig. 5.4. The Airy function for different amplitude reflectances r.

The intensity transmittance T_I of the Fabry–Perot interferometer, consisting of two mirrors a distance L apart, thus is given by

$$T_I = \frac{I_t}{I_e} = \frac{1}{1+K\sin^2 kL}. \tag{5.17}$$

This function is called the Airy function (Fig. 5.1). We observe that the function is periodic both in L and in k. For instance, if we keep L fixed and alter the wave number $k = 2\pi/\lambda$ or the wavelength λ, then we periodically observe the same intensity transmittance. In particular, because of the roots of the sine function we periodically obtain a transmission of unity, that is, complete transmission for certain wavelengths or frequencies. Therefore the instrument is wavelength selective (frequency selective) and represents an optical filter. Because of the periodicity of the transmitting regions it is a comb filter.

The complete transmission through both mirrors, when the distance between them is $n \cdot \lambda/2$, is highly surprising in view of the high reflectivity of each mirror, 99.9% say. Figure 5.5 demonstrates this peculiar behavior with two experimental arrangements. If just one mirror with a reflectance of 99.9% is placed in front of the detector, then only 0.1% of the incoming light reaches the detector. When a second mirror, again of 99.9% reflectance, is placed in between at a distance of $n \cdot \lambda/2$ from the

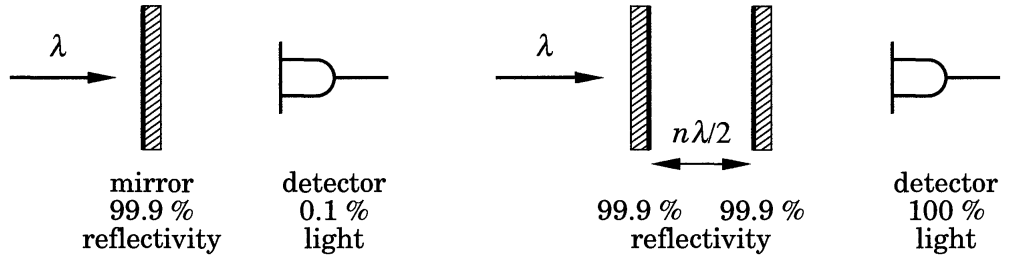

Fig. 5.5. Arrangement for demonstrating the reflection properties of one and of two mirrors.

first one, then not 0.1% of the 0.1% transmitted in the first arrangement is measured, but a full 100% of the incident light is detected, as if neither mirror were present. The actual action as a mirror depends on the experimental arrangement. Thus, an absolute value of reflectance cannot be ascribed to a mirror. A mirror can alter its reflection properties without being altered itself!

Figure 5.1 shows the dependence of the Airy function on the quantity kL for different amplitude reflectances r. For values of r near unity, sharp transmission regions are obtained. The distance between the maxima is of practical importance. The wavelength where complete transmission is observed is not unique, because every wavelength λ_n that obeys the equation

$$n\pi = k_n L = \frac{2\pi}{\lambda_n} L \qquad \text{or} \qquad n\frac{\lambda_n}{2} = L, \quad n \text{ integer}, \tag{5.18}$$

is completely transmitted. Thus, only the wavelength region between two successive maxima is of interest. This distance is usually given as a frequency difference $\Delta\nu$ and is called the free spectral range (FSR). Its size may be obtained in the following way. Two adjacent maxima of transmission at wave numbers k_n and k_{n+1} obey the relation (5.18) for the integers n and $n+1$, respectively. Subtracting both equations leads to

$$\pi = (k_{n+1} - k_n)L = \Delta k L = \frac{2\pi\,\Delta\nu}{c} L,$$

where additionally $\Delta\nu = (c/2\pi)\Delta k$ has been used. Thus, the free spectral range is given by

$$\Delta\nu = \frac{c}{2L}. \tag{5.19}$$

Two frequencies whose separation is smaller than $\Delta\nu$ can be distinguished unambiguously (within the resolving power of the instrument). The absolute wavelengths must be determined otherwise, at least to an accuracy of a free spectral range.

A second characteristic number of a Fabry–Perot interferometer is its finesse F. It indicates how many spectral lines are resolvable within a free spectral range, and is defined as

$$F = \frac{\Delta\nu}{\nu_\mathrm{h}}, \tag{5.20}$$

$\Delta\nu$ being the free spectral range and ν_h the width at half maximum of the Airy function peaks (see Fig. 5.1). The width ν_h is defined as the full frequency width of a region, where the intensity transmittance T is larger than 1/2. As can be seen by the example with $r = 0.2$ in Fig. 5.1, ν_h and therefore also the finesse F are defined for sufficiently large r only. But just these cases are of interest.

The width ν_h depends on the parameters r and L of the interferometer in the following way. A wave number k'_h is introduced by

$$k'_h L = \frac{2\pi\nu'_h}{c} L = \frac{\pi\nu_h}{c} L, \tag{5.21}$$

where $2\nu'_h = \nu_h$; ν'_h is the frequency width from the maximum to the half maximum. Then, from (5.17), we have (T_h = half of full transmission =1/2)

$$T_h = \frac{1}{2} = \frac{1}{1 + K \sin^2 k'_h L} . \tag{5.22}$$

For this relation to be valid requires

$$K \sin^2 k'_h L = 1 .$$

For $r \lesssim 1$ the transmission regions are small and therefore $k'_h L$ is also small. Then, $\sin(k'_h L)$ can be replaced by $k'_h L$, and we get

$$K(k'_h L)^2 = 1 \quad \text{or} \quad k'_h L = \frac{1}{\sqrt{K}} .$$

Together with (5.21) we have

$$k'_h L = \frac{\pi\nu_h}{c} L = \frac{1}{\sqrt{K}} \tag{5.23}$$

or

$$\nu_h = \frac{c}{\pi L\sqrt{K}} = \frac{c(1-r^2)}{\pi L 2r} . \tag{5.24}$$

This is the desired relation for ν_h. Then, using the definition (5.20) together with (5.19) and (5.24), we can express the finesse F by

$$F = \frac{\Delta\nu}{\nu_h} = \frac{c\pi L 2r}{2Lc(1-r^2)} = \frac{\pi r}{1-r^2} . \tag{5.25}$$

From this equation it follows that the number of resolvable spectral lines depends solely on the reflectance r of the mirrors; the larger it is, the higher the reflectance. A Fabry–Perot interferometer with $F = 100$ already is a good instrument; $F = 10000$ is possible at present and is commercially available.

A further important quantity is the resolving power A. As with every spectral instrument, it is defined by

$$A = \frac{\nu}{\nu_h} , \tag{5.26}$$

ν being the (mean) frequency and ν_h the full width at half maximum of a single transmission region, also called the instrumental linewidth. From the definition $F = \Delta\nu/\nu_h$ we have

$$\nu_h = \frac{\Delta\nu}{F} , \tag{5.27}$$

and thus obtain for the resolving power of a Fabry–Perot interferometer:

$$A = \frac{\nu}{\Delta\nu} F \,. \tag{5.28}$$

With this simple instrument, composed of just two plane parallel mirrors, astonishing values for the resolving power are attainable. A typical value for A is 10^8! A comparison with a grating spectrometer puts this figure into perspective. A grating with 1000 lines gives a resolving power of only 10^3 in the first diffraction order. However, the free spectral range of a Fabry–Perot interferometer is much smaller than that of a grating spectrometer.

5.2 Mode Spectrum of a Laser

A laser consists of several parts, one being a resonator to feed back part of the generated light into the amplifying medium. In the simplest case, the resonator consists of two plane parallel mirrors at a distance L. Without the laser material in between this is just the Fabry–Perot arrangement. The reflectance, however, is usually different for both mirrors, near 100% for the first one and significantly less for the second one, the output mirror (about 96% for a He–Ne laser). A resonator of this kind has a longitudinal mode spectrum similar to the line spectrum of a Fabry–Perot instrument. The spectral width of a laser line usually comprises several longitudinal modes of the laser resonator. Those modes that are sufficiently amplified by the laser medium are generated and radiated (Fig. 5.2).

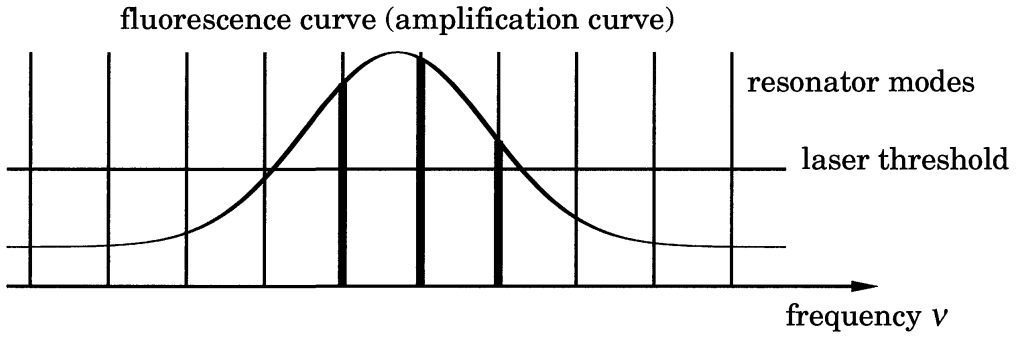

Fig. 5.6. The formation of the spectrum of laser light.

Thus, laser light gets its properties by multiple-beam interference. Several methods are available for measuring the mode spectrum of a laser. We put forward two of them: interference spectroscopy and difference-frequency analysis with fast photodiodes.

5.2.1 Interference Spectroscopy

When high resolving powers are needed in optics, it is usually the Fabry–Perot interferometer that is used. It is best suited for the determination of the mode spectrum of a laser. The arrangement is as follows (Fig. 5.7). The laser light is made slightly divergent by a lens, L_1, and enters the

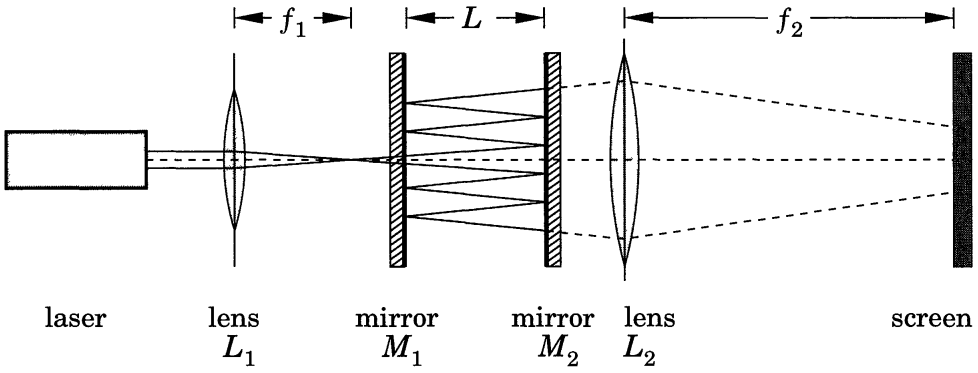

Fig. 5.7. Arrangement for the determination of laser modes with a Fabry–Perot interferometer.

Fabry–Perot interferometer, where the light is reflected back and forth between the two mirrors M_1 and M_2. The output light is collected by a lens, L_2, and directed onto a screen located in the back focal plane of the lens L_2. Thereby, all rays leaving the interferometer at the same angle are collected in one point. Why do we need lens L_1? Most lasers have an extremely small angle of divergence. It then becomes difficult to adjust the instrument to let even one laser mode pass the instrument. However, when we produce a set of oblique rays with lens L_1, different path lengths become available. At an angle of incidence α (Fig. 5.2.1) we have:

$$L_\alpha = \frac{L}{\cos\alpha}. \tag{5.29}$$

If the angle $\alpha = \alpha_{\mathrm{FSR}}$ is such that

$$\frac{L}{\cos\alpha_{\mathrm{FSR}}} = L + \frac{\lambda}{2}$$

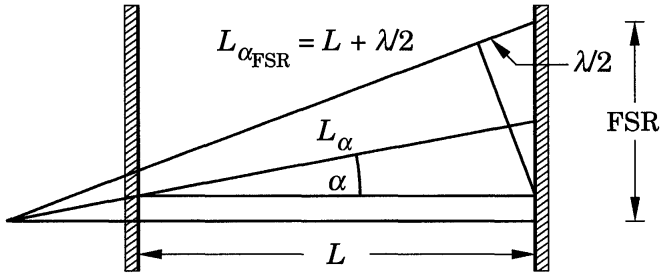

Fig. 5.8. Ring formation at the output of a Fabry–Perot interferometer.

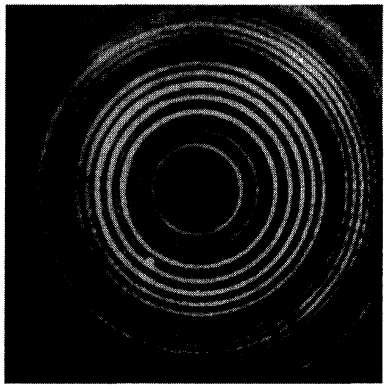

Fig. 5.9. Fabry–Perot ring system with five modes of a 15 mW He–Ne laser.

then the same wavelength λ is transmitted again. A particular wavelength λ from a divergent light beam thus leaves the instrument at discrete angles, for instance, at $\alpha = \alpha_0, \alpha_0 + \alpha_{\mathrm{FSR}}, \ldots$. Because of the rotational symmetry a ring system is obtained on the screen. If the divergent beam contains not just one but several modes, then each of them leads to a separate concentric ring system, $\alpha_\lambda, \alpha_\lambda + \alpha_{\mathrm{FSR}}, \ldots$, shifted by an angle α_λ according to the wavelength (Fig. 5.9).

The meaning of the free spectral range $\Delta\nu$ (or $\Delta\lambda$, or $\Delta\alpha$) is immediately detectable in the ring system. The separation of spectral lines can be determined only within a free spectral range. It is even necessary to know beforehand that the separation is smaller than the free spectral range to arrive at the correct value. The free spectral range can be altered by adjusting the mirror separation L. A smaller L leads to a larger $\Delta\nu$. Absolute wavelengths normally cannot be measured with a Fabry–Perot interferometer. Instead, it is very well suited for measuring difference frequencies, such as the splitting of spectral lines and differences of laser modes (Fig. 5.9) down to the MHz region. There, electronic devices take over for lower frequencies.

A different solution for observing laser modes is depicted in Fig. 5.10: the scanning Fabry–Perot interferometer. The light propagating along

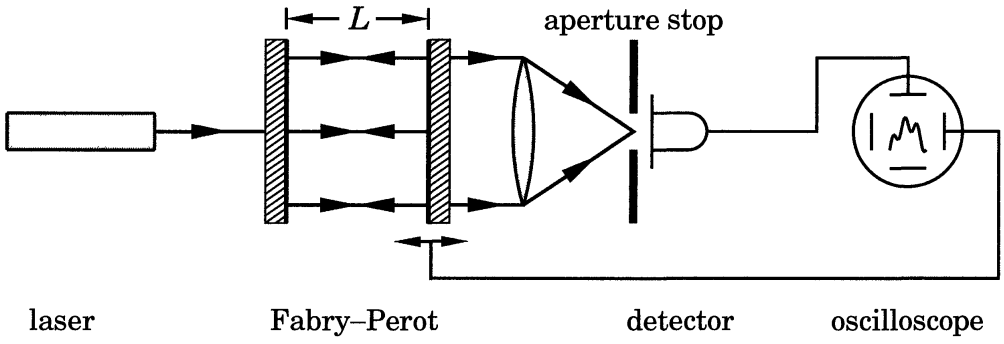

Fig. 5.10. Principle of the scanning Fabry–Perot interferometer.

the optical axis of a Fabry–Perot interferometer is collected and directed onto a photodiode. To shift different wavelengths into the transmission region, the length L between the mirrors is altered, usually piezoelectrically, and the photodiode signal (y-axis) is plotted versus the mirror separation (x-axis) on an oscilloscope. If the wavelength of the incident light is λ, then transmission is obtained at mirror separations of $\ldots, (n-1)\cdot\lambda/2, n\cdot\lambda/2, (n+1)\cdot\lambda/2, \ldots$. Again there is ambiguity because of the finite free spectral range according to $\Delta L = \lambda/2$ (Fig. 5.11). If more lines are present, they are transmitted at the corresponding lengths L_λ and form additional signals on the oscilloscope. Figure 5.12 shows three photographs taken from an oscilloscope screen. Three different He–Ne lasers with two, three, and five longitudinal modes have been analysed.

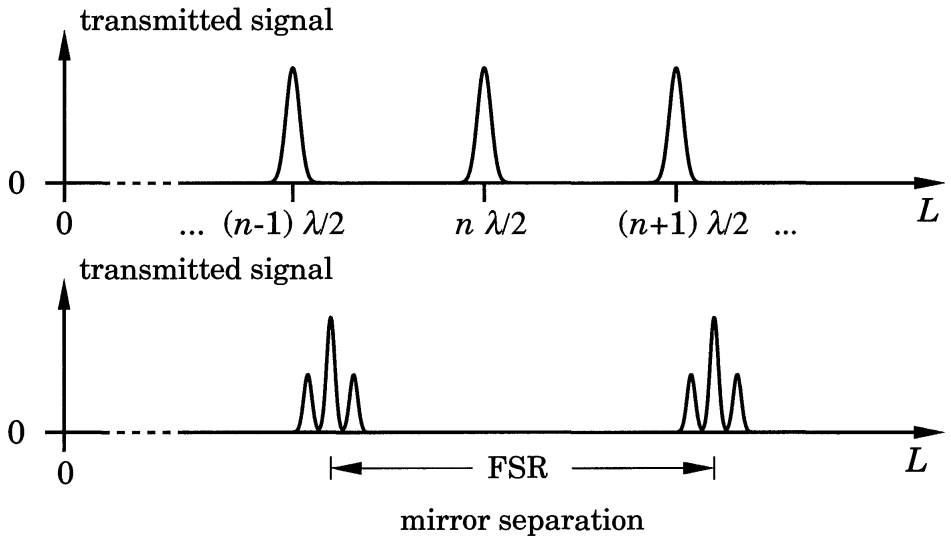

Fig. 5.11. Sketch of signals obtained with a scanning Fabry–Perot interferometer on an oscilloscope for light of one wavelength only (*above*) and for a laser with three modes (*below*). The repetition of the signal groups appears because the length L is varied over more than one free spectral range.

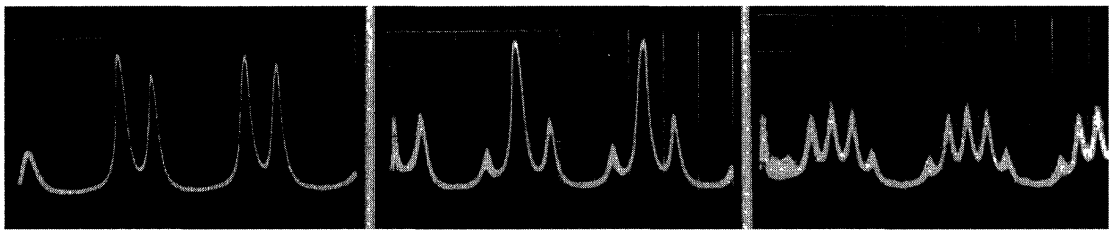

Fig. 5.12. Photographs from an oscilloscope screen showing the mode spectrum of three different He–Ne lasers with two, three, and five modes, respectively.

5.2.2 Difference-Frequency Analysis

Light intensities can be measured with a photodiode. For a large range of intensities, the number n_i of photoelectrons is proportional to the intensity

$$n_i \propto I = |E|^2 . \tag{5.30}$$

After amplification, a photocurrent is obtained that can be transformed into a voltage U,

$$U \propto n_i \propto I , \tag{5.31}$$

and plotted on the screen of an oscilloscope (Fig. 5.2.2).

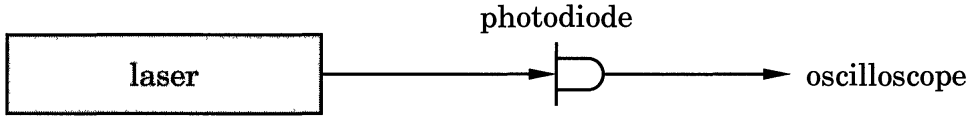

Fig. 5.13. Capturing laser light with a fast photodiode.

Photodiodes with response times in the subnanosecond region are commercially available. The oscillation of a light wave having a frequency of about 10^{15} Hz in the visible part of the spectrum cannot be resolved this way, but sufficiently low difference frequencies from a mixture of waves, as usually emitted by a laser, can be detected. The superposition of different frequencies leads to beats and thus to a time-dependent intensity that can be followed with sufficiently fast photodiodes.

Let $E(t)$ be the field amplitude of the superposition of two waves of circular frequencies ω_1 and ω_2:

$$E(t) = \exp(-i\omega_1 t) + \exp(-i\omega_2 t) . \tag{5.32}$$

Then, the dependence of the photocurrent and therefore the voltage U on time is

$$U(t) \propto I = 2 + 2\cos[(\omega_1 - \omega_2)t] . \tag{5.33}$$

Figure 5.14 shows the time-dependent intensity (short-term intensity) for two He–Ne lasers of different resonator lengths. From the period of the oscillation, the mode separation and thus the resonator length can be obtained.

Today's electronic frequency analysers allow the immediate display of the frequencies contained in a signal on an oscilloscope. Spectrum analysers are available for frequency ranges reaching some 10 GHz and thus are suitable for our present purpose. Figure 5.15 shows the screen of a

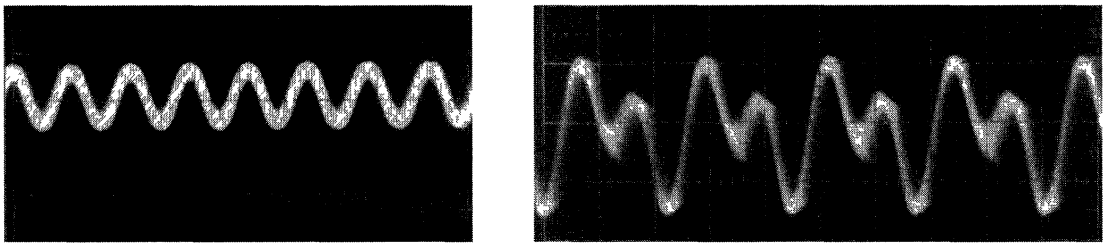

Fig. 5.14. Time-dependent intensity versus time for a 5 mW He–Ne laser (*left*) and a 15 mW He–Ne laser (*right*).

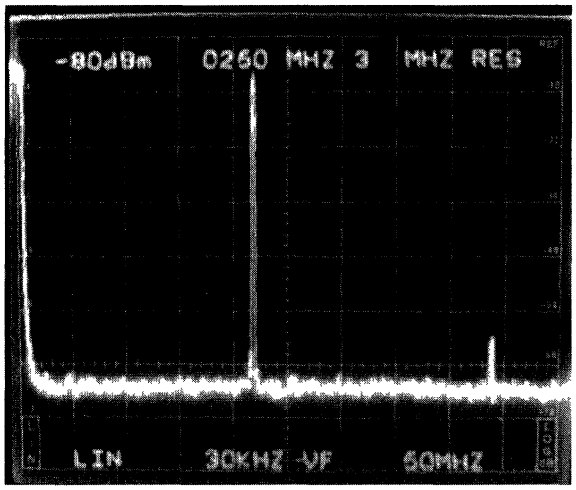

Fig. 5.15. Screen of a spectrum analyzer with an input signal from a He–Ne laser.

spectrum analyser with an input signal derived from the light of a He–Ne laser. The frequency is plotted along the horizontal axis. One horizontal division corresponds to 50 MHz. The amplitudes of the difference frequencies are plotted linearly along the vertical axis in arbitrary units. At the left margin, the zero frequency line is visible, added by the instrument. A strong difference frequency shows up at about $\nu = 220$ MHz, and a weak line at twice the frequency, 440 MHz. The laser thus emits three modes and has a resonator length of $L = c/2\Delta\nu = 68$ cm.

5.3 Dual-Recycling Interferometer

The Michelson interferometer has been used to show that the propagation velocity of light does not depend on the velocity of the light source itself and thereby initiated the theory of special relativity. Light again was used to prove the theory of general relativity through the deflection of light in the gravitational field of the sun. Gravitational fields even can form lenses for the light from stars or distant galaxies. These are stationary gravitational fields. The theory of general relativity, however, also predicts the existence of gravitational waves, that is, of propagating disturbances in

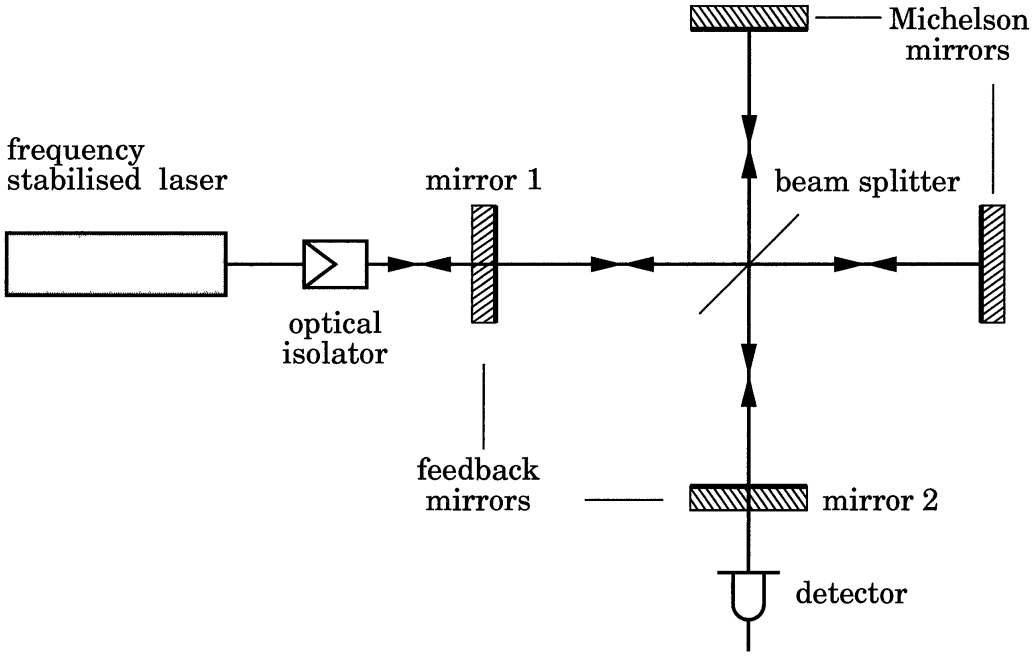

Fig. 5.16. Dual-recycling interferometer.

space–time. A direct measurement on earth has not yet been successfully performed, as the present gravitational wave detectors are not sensitive enough. A gravitational wave should alter the distances between objects, therefore interferometry suggests itself for measuring them, for instance, with the help of the Michelson interferometer. It transforms a distance variation from one arm of the interferometer into a phase shift of a light wave and, with the help of a reference wave from the other arm, into an intensity. In its basic configuration, where the phase shifted wave and the reference wave are superimposed only once, the Michelson interferometer is not sensitive enough. We know from the Fabry–Perot interferometer that the sensitivity can be improved substantially when multiple-beam interference is used. The question is, whether the increased sensitivity of the Fabry–Perot interferometer may be transferred to the Michelson interferometer. This is indeed possible. The Michelson interferometer has to be augmented by two additional mirrors placed at the entrance and exit of the instrument to "recycle" the (monofrequency) laser light to keep it for multiple interference (Fig. 5.16). We then have two crossed, coupled Fabry–Perot interferometers.

At first sight, it does not seem obvious that a mirror at the entrance of the interferometer should increase the sensitivity of the instrument, and even less obvious that a mirror in front of the detector should also increase the sensitivity. To understand this we need a closer look at some properties of the Michelson and the Fabry–Perot interferometer. We start with the Michelson interferometer. Suppose we use a monofrequency light wave of wavelength λ and shift one mirror by $\lambda/4$ from the balanced po-

sition. Then, the additional light path amounts to $\lambda/2$, and the detector gets no light, as both waves interfere destructively. What happens to the energy from the two waves? It is reflected back into the laser. The reflection of the incoming wave can be shown experimentally by placing a beam splitter in front of the interferometer to deflect part of the reflected light. Then a maximum in the amount of reflected light is measured when the detector at the output gets no light. A Michelson interferometer in this state of operation acts as a 100% reflector.

This reflector is now used as one mirror of a Fabry–Perot interferometer. The second mirror is placed in front of it and serves as the "recycling" mirror at the input of our Fabry–Perot interferometer (mirror 1 of Fig. 5.16). Control electronics with piezoelements are used to ensure that the Michelson interferometer stays in the state of 100% reflectance for the laser wavelength used. Then the sensitivity of the Fabry–Perot interferometer is transferred to the Michelson interferometer. The same argument can be used a second time for the light that has been generated by the action of a gravitational wave, leading to modulation of the incident laser light.

Systems with "dual recycling", as shown in Fig. 5.16, are presently being developed. Difficulties arise with the long interferometer arms with respect to vibration isolation, active control of the mirrors, control of heat expansion and contraction, etc. Nevertheless, astrophysicists hope to open up a new window to the universe with this instrument.

Problems

5.1 A Fabry–Perot interferometer has a finesse of $F = 10000$ and a mirror separation of $L = 5$ cm. Calculate the mirror recflectance r, the free spectral range $\Delta\nu$, the width ν_h of a spectral line and the resolution A of this instrument at $\lambda = 500$ nm. Can it be used to resolve two spectral lines at 516.7 nm and 516.9 nm unambiguously?

5.2 Calculate the amplitude reflectance R of a Fabry–Perot interferometer in a way analogous to the derivation of the transmittance T given in the text (sum over partial waves). Verify that energy conservation holds: $|T|^2 + |R|^2 = 1$.
Hint: the phase of the partial wave reflected back at the entrance mirror is shifted by π with respect to all remaining partial waves that contribute to the reflected wave.

5.3 Determine the finesse of a Michelson interferometer.

5.4 A Fabry–Perot interferometer with finesse $F = 1000$ is tuned for maximum transmission at the wavelength $\lambda = 632.8$ nm. By what amount has the mirror separation to be changed for the output intensity to drop to one half of its maximum value? How large is the corresponding displacement for a Michelson interferometer?

5.5 A plane, harmonic light wave with intensity I_e is incident on a Fabry–Perot interferometer parallel to the optical axis. Calculate the wave field and the energy density within the resonator for both minimum and maximum transmission T. To do so, represent the field in the resonator cavity as a superposition of a forward and a backward traveling harmonic wave, and use Stokes' formulae $r' = -r$ and $tt' = 1 - r^2$. Here, r and r' are the amplitude reflectances upon reflection of a wave coming from outside the instrument and from within the instrument, respectively; t and t' are the corresponding amplitude transmittances.

5.6 Determine the frequency separation of the longitudinal modes of a He–Ne laser ($\lambda = 632.8$ nm) having a resonator length of 60 cm. Repeat this calculation for a semiconductor laser having a resonator length of 0.5 mm, and an index of refraction of $n = 3.6$, emitting at $\lambda = 1.55$ μm. The light of the He–Ne laser is analyzed by using a fast photodiode with linear characteristic, $U \propto I(t)$; $I(t)$ being the short-term intensity. Assume that in the He–Ne laser three adjacent modes are excited with an amplitude ratio of 1:2:1. Give the frequencies and relative amplitudes of the harmonic components of the photocurrent.